



DOI: 10.34910/MCE.103.3

Reinforced concrete beams strength under power and environmental influences

N.V. Frolov*, G.A. Smolyago

Belgorod State Technological University named after V.G. Shukhov, Belgorod, Russia

**E-mail: frolov_pgs@mail.ru*

Keywords: durability, reinforced concrete beams, experimental investigations, bending strength, corrosion damages, mechanical properties, load

Abstract. The article is devoted to the problem of assessing and predicting the strength of normal sections of bended reinforced concrete elements, which are exposed during operation to long-term force and environmental influences. It is noted that together with the accumulation of concrete and steel reinforcement corrosion damages, the load bearing capacity of reinforced concrete structures can be significantly reduced. At the same time, the existing methods for strength calculating are still applied and do not allow from a single point of view to reflect sufficiently strictly and in detail the stress-strain state of normal sections of bended reinforced concrete elements, taking into account the influence of all operational factors on it. Thereby, based on the nonlinear deformation model of reinforced concrete, a universal calculation procedure was developed. To approve it, the experimental studies of reinforced concrete beams samples that were under static load in sulfate- and chloride-containing aggressive environments for a long time were carried out. New features of corrosion damages accumulation in concrete and steel reinforcement in these aggressive environments were determined. After comparing the experimental and calculated data of normal sections strength, it was concluded that the proposed method has sufficient accuracy and can be used for practical calculations of operated bended reinforced concrete elements with defects and damages.

1. Introduction

In many cases, during long-term operation, bended reinforced concrete elements, in addition to power loading, also perceive various aggressive environmental influences, which lead to corrosion initiation and, as a result, to concrete and reinforcement damages. Over time, together with corrosion damages accumulation, a significant decrease in bearing capacity of reinforced concrete structures can occur. In this regard, to ensure bended reinforced concrete elements durability and reliability during operation under load in aggressive environments, in our opinion, the valuation and prediction researches of their normal sections strength are relevant.

Despite the broad theoretical and experimental researches of bended reinforced concrete elements under various operating conditions, presented in publications [1–8], far from all the features of the stress-strain state of their normal sections are studied with the long-term joint force and environmental influences.

Based on scientific literature general analysis of corrosion damages development in reinforced concrete structures [9–17], it can be noted that among a wide range of environmental influences, the effects of sulfates are most aggressive with respect to concrete with a cement binder, and chloride effects with respect to steel reinforcement. As a result of corrosion damages, the sections geometric dimensions decrease and the deformation-strength characteristics of concrete and steel reinforcement decrease. In addition, breaking adhesion between concrete and reinforcement is possible [18, 19].

It was determined that corrosion damages accumulation of concrete and reinforcement in reinforced concrete structures often proceeds jointly and depends on the sign and level of stresses acting in the materials [20, 21]. But taking into account such temporary factors as strength set and concrete creep in bended concrete elements researches, these processes are considered superficially.



The most methods and approaches to solving problems of determining the normal sections strength of bended reinforced concrete elements with damages were developed before the computer technology existed. The lack of powerful computing tools forced scientists to go through the development of the so-called engineering methods of calculation [22–25]. However, such a path led to fragmented decisions, dividing the definition domain into a number of sections with different models and solutions, loading with empirical coefficients, and the need to correct them when expanding the types of materials and accumulating information about their work.

It was determined in [26] that structural materials degradation properties as a result of long-term force impacts can be calculated in reinforced concrete model deformation by adjusting the corresponding deformation diagrams and section sizes. At the same time, the existing calculation methods based on the deformation model make it possible to determine the normal sections strength of bended reinforced concrete elements with only corrosion damages of longitudinal reinforcement and concrete of the compressed zone [27–29, 33]. Concrete damages in the stretched zone and at the section side faces are outside of consideration. In addition, a linear, and even uniform damage plot is allowed for all sections, which cannot be linked in any way with a different level of stress distribution in different sections of the element, or with cases of uneven concentration of an aggressive medium over the span. Thus, these techniques do not allow, from a single point of view, to reflect in sufficient detail and objectively the stress-strain state of normal sections of bended reinforced concrete elements under prolonged force and environmental influences.

The purpose of this article is the development and experimental approval of a universal method for calculating the strength of normal sections of bended concrete elements subjected to prolonged force and environmental influences.

To achieve this goal, a number of tasks are solved:

- calculating method development for normal sections strength of bended reinforced concrete elements under long-term force and environmental influences, taking into account non-linear diagrams of concrete deformation and various schemes of corrosion damages development at the section boundaries, as well as various sections damage degrees within the span;
- conducting experimental researches of normal sections strength of bended reinforced concrete elements which were under load in aggressive environments for a long time;
- developed methodology verification by comparing theoretical and experimental data on normal sections strength of bended reinforced concrete elements with corrosion damage.

2. Method

2.1. Calculation method

The calculation method is based on a deformation model of reinforced concrete taking into account the following premises, working hypotheses and assumptions:

- The normal section is taken for calculation, the stress-strain state of which corresponds to the average state of the block between cracks;
- At all levels of element loading, the compatibility conditions of structural materials deformations and the hypothesis of flat sections remain valid for the section under consideration;
- The magnitude of the external load on the element and aggressive medium concentration near the section are considered constant throughout the entire observation period; environmental influences begin to appear with a relatively stable stress-strain state of the cross section;
- The kinetic stability of nonequilibrium processes of corrosion damage promoting and creep deformations development is accepted;
- Only concrete decaying corrosion damages with a kinetics parameter $m = 1$ [30, 31] is considered, the measure of which in the calculation is the damage depth, determined according to the expression V.M. Bondarenko:

$$\delta(t, t_0) = \left(1 - \Delta\delta(t, t_0) \cdot e^{-\alpha(t-t_0)}\right) \delta_{cr}(t_0), \quad (1)$$

and nonlinear function of the damage coefficient $K^*(z)$, determined from the boundary conditions according to Fig. 1. For the concrete surface layer ($z = 0$), the damage coefficient K^*_{min} is found in accordance with Russian State Standard GOST 25881. Hereinafter, designations with the symbol "*" refer to materials damaged by corrosion.

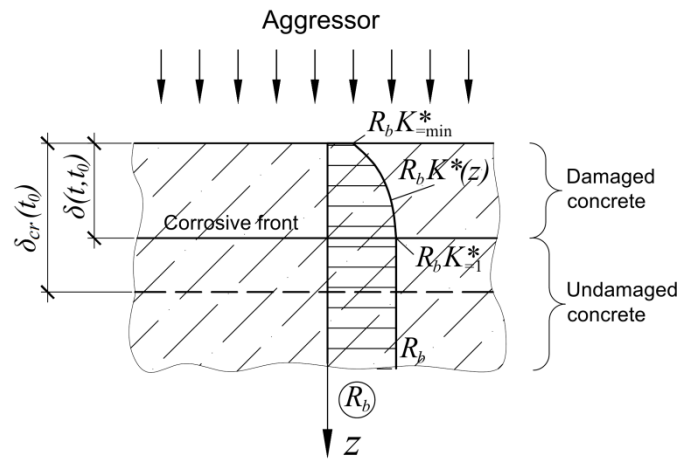


Figure 1. Concrete corrosion damages.

The following notation is introduced in formula (1) and in Fig. 1: $\delta_{kp}(t_0)$ and α are the kinetics parameters of concrete corrosion damages, determined from experimental data; $\Delta\delta(t, t_0)$ is the relative deficit of the current value of corrosion damage depth $\delta(t, t_0)$; t and t_0 are current and initial observation period, respectively; R_b is a characteristic of concrete mechanical properties, in this case is prism strength;

- Steel reinforcement corrosion damages is taken into account by a decrease in the calculated cross-sectional area according to the formula

$$A_s^* = A_s - A_s^{cor}, \quad (2)$$

where A_s^{cor} is lost area, determined by the Table 1 depending on the reinforcing bars wear model; reinforcement damage depth is determined by the formula

$$\delta_s(t) = \begin{cases} 0, & t \leq t_{inc} \\ \frac{\delta_{s,0} \cdot (t - t_{inc})}{T + (t - t_{inc})}, & t > t_{inc} \end{cases}, \quad (3)$$

where: t_{inc} is reinforcement corrosion initiation time, found from the expression (1) with concrete damage depth equal to the thickness of the protective layer; $\delta_{s,0}$ and T are the parameters of the kinetics of corrosion damages of steel reinforcement, determined from experimental data.

Table 1 shows the main models of corrosion damage development along the cross section of a steel reinforcing bar. The model "continuous uniform corrosion" assumes that the aggressive conditions on the entire surface of the cross section of the rod are the same and its damages along the perimeter will be uniform with the depth δ_s . The models of "uneven corrosion" suggest that on one of the surfaces of the rod cross-section (in this case, on the bottom) the conditions are much more aggressive than on others, while its damage will be uneven with a maximum depth of δ_s . So, in the "pitting corrosion" model, the damage boundary is described by a circle curve with a radius δ_s and a with a center located in the corrosion area. In the "flat front" model, the damage boundary is described by a straight line outlying to distance δ_s from the corrosion area. In the "sickle-shaped front" model, the damage boundary is described by an arc with three parametric points, which are determined using the sector angle α and ordinate δ_s from the corrosion area;

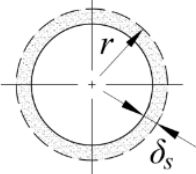
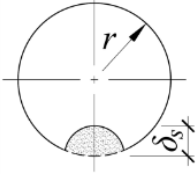
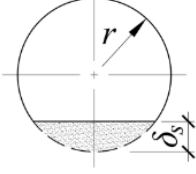
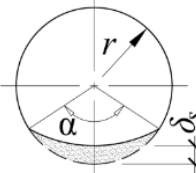
- Diagrams of concrete deformation under short-term and long-term loading (Fig. 2) are described by a power polynomial of the form

$$\sigma_b = \sum_{k=1}^n a_k \varepsilon_b^k, \quad (4)$$

where: a_k is polynomial coefficients determined experimentally or by calculation, depending on the loading mode; k is an exponent equal to positive integers 1, 2 ... n . In this case, the value of n is taken based on the type of design diagram of concrete deformation, for example, for a nonlinear diagram with a descending branch $n = 5$.

The parameters of concrete deformation graphs under tension are determined experimentally or based on the corresponding parameters in compression using empirical dependence between them.

Table 1. Models of reinforcement bar corrosion wear.

Bar corrosion wear model	Reinforcement bar cross section	
	Design model	Calculated area of corrosion damage A_s^{cor}
Uneven corrosion	Continuous uniform corrosion 	$\pi\delta_s(2r - \delta_s)$
	Pitting corrosion [Shmelev, G.D] 	$\delta_s^2\sqrt{m-m^2} + \delta_s^2 \arcsin\sqrt{m} - 2r\delta_s\sqrt{m} +$ $+ \delta_s\sqrt{mr^2 - \delta_s^2m^2} + r^2 \arcsin\frac{\delta_s\sqrt{m}}{r},$ where $m = 1 - \delta_s^2 / 4r^2$
	Flat front 	$(\delta_s - r)\sqrt{2r\delta_s - \delta_s^2} + r^2 \arcsin\frac{\sqrt{2r\delta_s - \delta_s^2}}{r}$
	Sickle-shaped front [Ovchinnikov, I.G.] 	$\frac{r^2}{2}(\alpha - \sin\alpha) + \frac{(2r - \delta_s)^2}{2}\left(\frac{\alpha}{2} - \sin\frac{\alpha}{2}\right),$ where $\alpha = 4 \arccos\left(1 - \frac{\delta_s}{2r}\right)$

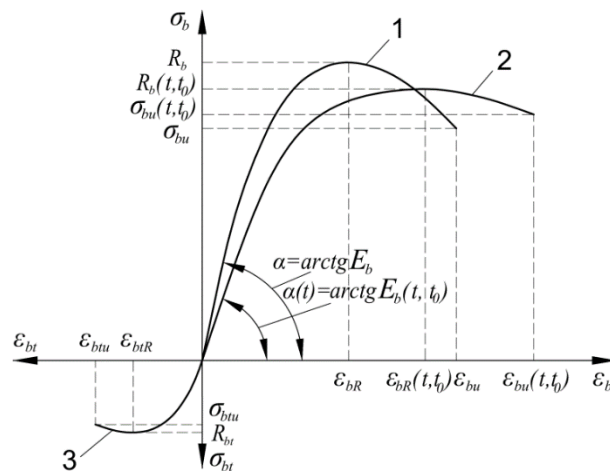


Figure 2. Concrete deformation diagrams under short-term (1, 3) and long-term (2) loadings.

Changes in concrete deformation diagrams parameters due to corrosion are taken into account using the damage coefficient K^* .

- After the concrete stretching deformations reach their limit values ϵ_{btu} , the stress diagram obtains a rectangular shape with the ordinate $\psi_{bt}R_{bt}$, where the coefficient ψ_{bt} takes into account the gradual decrease in the strength resistance of concrete of the stretched zone after crack formation and is determined based on studies [32] depending on the magnitude of the stresses acting in the tensile reinforcement according to the formula

$$\psi_{bt} = \left\{ \begin{array}{l} \psi_{bt,1} = e^{\frac{1}{k_1 k_2} \times \frac{\varepsilon_{btu} - \varepsilon_{bt}}{\varepsilon_{btu}} \sum_{j=1}^m \frac{n_j d_j}{h_{0j}}}, \text{ at } \sigma_s < \sigma_{sy} \\ \psi_{bt,2} = \psi_{bt,1} = \text{const}, \text{ at } \sigma_s = \sigma_{sy} \\ \psi_{bt,3} = \psi_{bt,2} \frac{\varepsilon_{bt, \sigma_{sy}}}{\varepsilon_{bt}}, \text{ at } \sigma_s = \sigma_{sy} \end{array} \right. \quad (5)$$

where: k_1 is the number of armature rows; k_2 is the coefficient taking into account the armature profile; ε_{btu} is concrete stretching ultimate strains; ε_{bt} , ε_{bt} , σ_{sy} is the most stretched concrete fiber deformations, respectively, at the current value of stresses in the armature and at the moment of its transition to strengthening; n_j is the number of bars of the same diameter; d_j , h_{0j} is respectively the diameter of the j -th bar and the distance from its center of gravity to the most compressed concrete fiber.

- Steel reinforcement deformation diagrams under tension and compression, both for short-term and for long-term loading are piecewise linear.

Stress-strain determination state and normal section strength of flexural element is carried out according to Fig. 3.

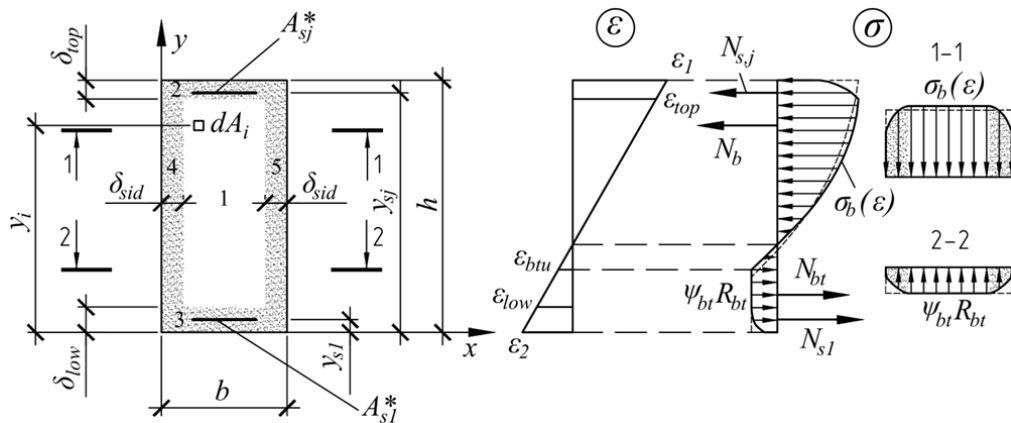


Figure 3. The stress-strain state of the normal section: 1 is the number of the characteristic undamaged area; 2, 3, 4, 5 are the numbers of characteristic damaged areas; δ_{top} , δ_{low} , δ_{sid} is the depth of concrete damage at the upper, lower and side faces, respectively; y_i , y_{sj} is the distance from the lower face of the section, respectively, to the elementary concrete ground dA_i and to the center of gravity of the section of steel reinforcement A_{sj}^* .

The calculated cross section is represented as the sum of elementary layers with a thickness of dy . For each characteristic section, the area of this layer, which has an even distribution of stresses along the width b_n , is $dA_b = b_n dy$, where n is parcel number. The designation of the relative section height to the elementary layer is introduced $\zeta_i = y_i / h$. With this in mind, for a section without cracks, the equations of equilibrium of longitudinal forces and moments have the form

$$\begin{aligned} & (b - 2\delta_{sid})h \int_{\delta_{low}/h}^{(h-\delta_{top})/h} \sigma_{b1}(\varepsilon) d\xi + bh \int_{(h-\delta_{top})/h}^1 \sigma_{b2}(\varepsilon) d\xi + \\ & + bh \int_0^{\delta_{low}/h} \sigma_{b3}(\varepsilon) d\xi + 2h \int_{\delta_{low}/h}^{(h-\delta_{top})/h} \int_0^{\delta_{sid}} \sigma_{b4}(\varepsilon) dx d\xi + \sum_{j=1}^m \sigma_{sj} A_{sj}^* = 0; \end{aligned} \quad (6)$$

$$\begin{aligned} & (b - 2\delta_{sid})h^2 \int_{\delta_{low}/h}^{(h-\delta_{top})/h} \sigma_{b1}(\varepsilon) \xi d\xi + bh^2 \int_{(h-\delta_{top})/h}^1 \sigma_{b2}(\varepsilon) \xi d\xi + \\ & + bh^2 \int_0^{\delta_{low}/h} \sigma_{b3}(\varepsilon) \xi d\xi + 2h^2 \int_{\delta_{low}/h}^{(h-\delta_{top})/h} \int_0^{\delta_{sid}} \sigma_{b4}(\varepsilon) \xi dx d\xi + \sum_{j=1}^m \sigma_{sj} A_{sj}^* h \xi_{sj} - M = 0. \end{aligned} \quad (7)$$

The integrands $\sigma_{b,n}(\varepsilon)$, are functions of stress diagrams at characteristic parts of the section, equal to

$$\begin{aligned}\sigma_{b1}(\varepsilon) &= \sigma_b(\varepsilon), & \varepsilon_{low} \leq \varepsilon \leq \varepsilon_{top}; \\ \sigma_{b2}(\varepsilon) &= \left(\frac{\varepsilon - \varepsilon_{top}}{\varepsilon_1 - \varepsilon_{top}} \right)^2 \left(\sigma_{b,top}^*(\varepsilon_1) - \sigma_b(\varepsilon_{top}) \right) + \sigma_b(\varepsilon_{top}), & \varepsilon_{top} \leq \varepsilon \leq \varepsilon_1; \\ \sigma_{b3}(\varepsilon) &= \left(\frac{\varepsilon - \varepsilon_{low}}{\varepsilon_2 - \varepsilon_{low}} \right)^2 \left(\sigma_{b,low}^*(\varepsilon_2) - \sigma_b(\varepsilon_{low}) \right) + \sigma_b(\varepsilon_{low}), & \varepsilon_2 \leq \varepsilon \leq \varepsilon_{low}; \\ \sigma_{b4}(\varepsilon) &= -\frac{\sigma_b(\varepsilon) - \sigma_{b,sid}^*(\varepsilon)}{\delta_{sid}^2} x^2 + 2 \frac{\sigma_b(\varepsilon) - \sigma_{b,sid}^*(\varepsilon)}{\delta_{sid}} x + \sigma_{b,sid}^*(\varepsilon), & \varepsilon_{low} \leq \varepsilon \leq \varepsilon_{top}.\end{aligned}\quad (8)$$

After substituting (8) into (6-7) and transformations, equations are obtained which describe the stress-strain state of the cross section of a bended reinforced concrete element without cracks. Further, similar equations are obtained for the cases when cracks are formed and developed in height in damaged and healthy concrete of the stretched section zone. In general view, these equations are as follows

$$\frac{h}{\varepsilon_1 - \varepsilon_2} \left(N'_{b1} + N'_{b2} + N'_{b3} + 2N'_{b4} \right) + \sum_{j=1}^m \sigma_{sj} A_{sj}^* = 0; \quad (9)$$

$$\frac{h^2}{(\varepsilon_1 - \varepsilon_2)^2} \left(M'_{b1} + M'_{b2} + M'_{b3} + 2M'_{b4} \right) + \sum_{j=1}^m \sigma_{sj} A_{sj}^* h \xi_{sj} - M = 0, \quad (10)$$

here with the stresses in the reinforcement are determined according to the expression

$$\sigma_{sj} = f(\varepsilon_{sj}) = f \left[\varepsilon_2 + (\varepsilon_1 - \varepsilon_2) \xi_{sj} \right]. \quad (11)$$

Members of equation (9–10) are found for each characteristic part of section from the expressions

$$N'_{b1} = (b - 2\delta_{sid}) \left(\psi_{bt} R_{bt} (\chi_1 - \varepsilon_{low}) + \sum_{k=1}^n \frac{a_k}{k+1} (\varepsilon_{top}^{k+1} - \chi_1^{k+1}) \right); \quad (12)$$

$$N'_{b2} = b \cdot \frac{(\varepsilon_1 - \varepsilon_{top}) \left(\sigma_{b,top}^*(\varepsilon_1) + 2\sigma_b(\varepsilon_{top}) \right)}{3}; \quad (13)$$

$$N'_{b3} = b \left(\frac{\psi_{bt} R_{bt} \left(K_{low}^* + 2K_{low}^*(\chi_2) \right) (\chi_2 - \varepsilon_2)}{3} + \frac{(\varepsilon_{low} - \chi_2) \left(\sigma_{b,low}^*(\chi_2) + 2\sigma_b(\varepsilon_{low}) \right)}{3} \right); \quad (14)$$

$$N'_{b4} = \delta_{sid} \frac{1}{3} \left(\psi_{bt} R_{bt} \left(K_{sid}^* + 2 \right) (\chi_1 - \varepsilon_{low}) + \sum_{k=1}^n \frac{a_{k,sid}^*}{k+1} (\varepsilon_{top}^{k+1} - \chi_1^{k+1}) + 2 \sum_{k=1}^n \frac{a_k}{k+1} (\varepsilon_{top}^{k+1} - \chi_1^{k+1}) \right); \quad (15)$$

$$M'_{b1} = (b - 2\delta_{sid}) \left(\frac{\psi_{bt} R_{bt} (\chi_1 - \varepsilon_{low}) (\varepsilon_{btu} - 2\varepsilon_2 + \varepsilon_{low})}{2} + \sum_{k=1}^n \frac{a_k}{k+2} (\varepsilon_{top}^{k+2} - \chi_1^{k+2}) - \varepsilon_2 \sum_{k=1}^n \frac{a_k}{k+1} (\varepsilon_{top}^{k+1} - \chi_1^{k+1}) \right); \quad (16)$$

$$M'_{b2} = b (\varepsilon_1 - \varepsilon_{top}) \left(\frac{\varepsilon_1 \left(3\sigma_{b,top}^*(\varepsilon_1) + 3\sigma_b(\varepsilon_{top}) \right) + \varepsilon_{top} \left(\sigma_{b,top}^*(\varepsilon_1) + 5\sigma_b(\varepsilon_{top}) \right)}{12} - \varepsilon_2 \frac{\left(\sigma_{b,top}^*(\varepsilon_1) + 2\sigma_b(\varepsilon_{top}) \right)}{3} \right); \quad (17)$$

$$M'_{b3} = b \cdot \left(\frac{\psi_{bt} R_{bt} (K_{low}^* + 5K_{low}^*(\chi_2)) (\varepsilon_2 - \chi_2)^2}{12} + \frac{\varepsilon_{btu} (3\sigma_{b,low}^*(\chi_2) + 3\sigma_b(\varepsilon_{low}))}{12} + \frac{\varepsilon_{low} (\sigma_{b,low}^*(\chi_2) + 5\sigma_b(\varepsilon_{low}))}{12} - \frac{(\sigma_{b,low}^*(\chi_2) + 2\sigma_b(\varepsilon_{low}))}{3} \varepsilon_2 \right); \quad (18)$$

$$M'_{b4} = \delta_{sid} \frac{1}{3} \left(\frac{\psi_{bt} R_{bt} (K_{sid}^* + 2) (\chi_1 - \varepsilon_{low}) (\varepsilon_{btu} - 2\varepsilon_2 + \varepsilon_{low})}{2} + \sum_{k=1}^n \frac{a_{k,sid}^*}{k+2} (\varepsilon_{top}^{k+2} - \chi_1^{k+2}) - \varepsilon_2 \sum_{k=1}^n \frac{a_{k,sid}^*}{k+1} (\varepsilon_{top}^{k+1} - \chi_1^{k+1}) + 2 \sum_{k=1}^n \frac{a_k}{k+2} (\varepsilon_{top}^{k+2} - \chi_1^{k+2}) - 2\varepsilon_2 \sum_{k=1}^n \frac{a_k}{k+1} (\varepsilon_{top}^{k+1} - \chi_1^{k+1}) \right). \quad (19)$$

The parameters values χ_1 and χ_2 in (12-19) are determined based on the conditions:

- if $\varepsilon_2 < \varepsilon_{btu}$, there are no cracks in the concrete and $\chi_1 = \varepsilon_{low}$, $\chi_2 = \varepsilon_2$;
- if $\varepsilon_2 \geq \varepsilon_{btu}$, but $\varepsilon_{low} < \varepsilon_{btu}$, cracks are formed and developed only in corrosion-damaged concrete at the lower boundary of the cross section, and $\chi_1 = \varepsilon_{low}$, $\chi_2 = \varepsilon_{btu}$. In this case $\sigma_{b,low}^*(\chi_2) = \psi_{bt} R_{bt} K_{low}^*(\varepsilon_{btu})$;
- if $\varepsilon_{low} \geq \varepsilon_{btu}$, the cracks form and exit into the healthy concrete zone, and $\chi_1 = \varepsilon_{btu}$, $\chi_2 = \varepsilon_{low}$.

After the deformations representing of the concrete of the upper face through the curvature in the section $\varepsilon_1 = \mathcal{N} h + \varepsilon_2$ in equation (9), \mathcal{N} and ε_2 remain unknown. Determining the parameters of the cross section stress-strain state according to the given curvature values, the half-value method is used to find the value ε_2 and, accordingly, ε_1 . Further, from the equation (10), the bending moment M acting in the section is determined, the limiting value of which is equal to the normal section strength M_{ult} .

It should be noted that changing in Fig. 3 damaged areas to healthy ones, and changing the corresponding terms of equations (12–19), one can describe particular schemes of the approach of an aggressive environment with respect to a rectangular section.

2.2. Experimental research methods

The purpose of the experimental researches was to obtain the necessary data on the accumulation of concrete and steel reinforcement damage over time and their effect on the normal sections strength of bended reinforced concrete elements under prolonged power and environmental influences, allowing us to evaluate the proposed calculation method reliability.

Experimental researches were carried out in accordance with the developed program, which provides for testing reinforced concrete beams samples in an amount of 27 pcs. The samples were made of a rectangular cross-section of 60×100 (h) mm with a calculated span of $l_0 = 1400$ mm.

After manufacturing, all samples were stored for 28 days in one laboratory with normal temperature and humidity conditions, after which they were divided into one control (11 pcs.) and two main (8 pcs.) groups of twin beams. Then, the first series of tests of reinforced concrete beams with a short-term load on static bending before failure was carried out, which included three samples from control group, the results of which determined the actual value of the design breaking load P_u^{BK-0} . The remaining 24 samples were loaded and placed for a certain period of time in various environmental conditions.

The samples of the control group were in the same laboratory as during strength gain. Samples of the first and second main groups were respectively in sulfate and chloride containing aggressive media, artificially created in the room to accumulate corrosion damages of concrete and steel reinforcement.

The subsequent series of tests of reinforced concrete beams with a static bending load before failure included two samples from each group. Thus, four more test series of six samples of reinforced concrete beams were formed. In these experimental studies, the main variable parameter was the duration of power and environmental impacts on the samples, equal to 180, 360, 720 and 1080 days from the moment they gained design strength. The accepted samples marking of reinforced concrete beams and series numbers of their tests with load before failure are given in Table 2.

Table 2. Beams samples marking and the series numbers of tests with load before failure.

Sample group	Type of environment	Reinforced concrete beams samples marking, taking into account the impact duration and the number of the test series of the load before failure				
		0 days, series no. 1	180 days, series no. 2	360 days, series no. 3	720 days, series no. 4	1080 days, series no. 5
Control (BK)	Non-aggressive environment	BK-0-1	BK-180-1	BK-360-1	BK-720-1	BK-1080-1
		BK-0-2	BK-180-2	BK-360-2	BK-720-2	BK-1080-2
		BK-0-3				
Main no. 1 (BOS)	Sulphate aggressive environment	–	BOS-180-1	BOS-360-1	BOS-720-1	BOS-1080-1
		–	BOS-180-2	BOS-360-2	BOS-720-2	BOS-1080-2
Main no. 2 (BOH)	Chloride aggressive environment	–	BOH-180-1	BOH-360-1	BOH-720-1	BOH-1080-1
		–	BOH-180-2	BOH-360-2	BOH-720-2	BOH-1080-2
The number of samples in a test series		3	6	6	6	6

Reinforced concrete beams reinforcement was performed by flat single frames with working stretched reinforcement in the form of rods $\varnothing 8$ mm of A240 class. To ensure anchorage, the ends of the rods are brought out beyond the supporting section of the beams by 90 mm with a bend length of 70 mm. As compressed reinforcement, $\varnothing 4$ mm rods made of class B500 wire are structurally installed. The concrete protective layer for stretched and compressed reinforcement was adopted 10 mm. The transverse reinforcement is made in the form of clamps from rods $\varnothing 3$ mm of class A240, installed with a constant pitch of 40 mm. The reinforcement scheme of laboratory beams samples is shown in Fig. 4.

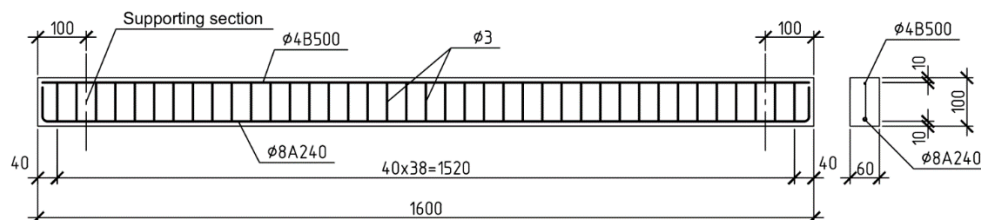


Figure 4. Reinforcement scheme for samples of reinforced concrete beams.

For all samples manufacture, concrete of class compressive strength B20 is used. At the same time, fine grinding sodium chloride (NaCl) in a ratio up to 5 % from cement weight was introduced into the concrete mixture intended for beams samples of the main group no. 2 (BOH). This did not lead to a significant decrease in the strength of concrete, but under wet conditions it contributed to steel reinforcement corrosion initiation.

After the first series of tests, based on the condition of the same rigidity, the remaining beams with the help of a hydraulic jack and a steel frame were pulled together in pairs by a force equal to $0.6P_u^{BK-0}$ (Fig. 5, a), which was further supported by ties. Force control was carried out using an exemplary compression dynamometer. The force transfer from the jack to the ties and, therefore, to the beams was carried out by uniformly nuts tightening at the ends of the ties with a torque spanner until the readings on the dynamometer decreased by 1 % or the total deflection of the beams increased by 0.01 mm, fixed by the dial indicator. The decrease in the ties force due to the corrosion damage development and the creep deformations growth was periodically replenished to the initial value. For this, two beams were again installed in a steel frame and reloaded with a jack with control of the force by a dynamometer. In this case, the force at which there was an increase in the total beams deflection by 0.01 mm was considered the total force acting at the moment in the ties. The real decrease in the load level of the beams during the tests did not exceed 5 %.

The design models for reinforced concrete beams during long-term tests and short-term load tests before failure are assumed to be the same: a single-span hinged-supported beam, loaded with two concentrated forces with the formation in clean bending zone of $0.164l_0$ a span (Fig. 5, b).

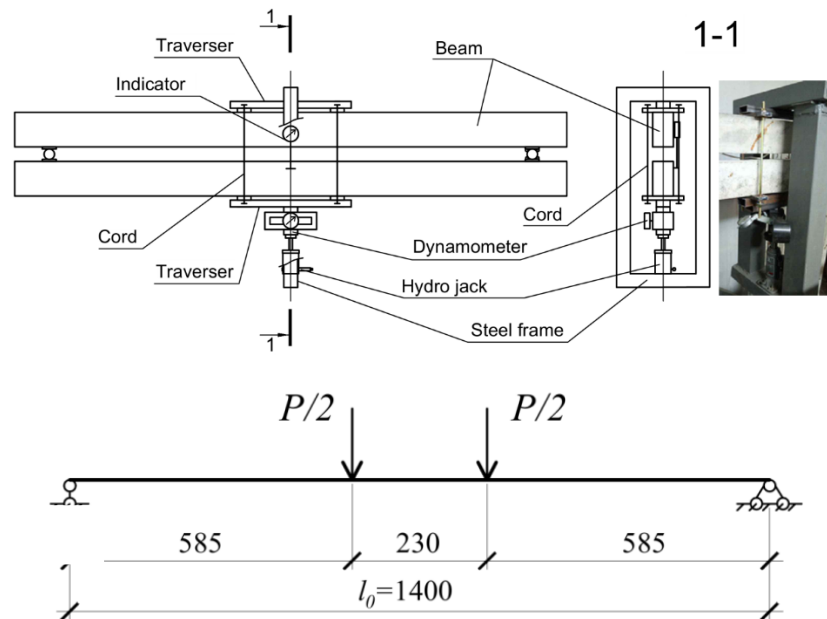


Figure 5. The principal (a) and calculated (b) loading scheme for reinforced concrete beams for long-time tests.

In order to initiate the development of corrosion processes in concrete and steel reinforcement, a special stand for long-term testing was made (Fig. 6). Its basic element was corrosion-resistant polymer baths with liquid electrolyte. A 2 % aqueous solution of sulphuric acid (H_2SO_4) was in one bath. It was intended to simulate a sulfate aggressive medium effect on the samples of BOS group, the other bath with distilled water was intended to simulate the effect of a chloride aggressive environment on the samples of BOH group containing an additive of sodium chloride (NaCl) in concrete. Using an electric telfer and rigging equipment, the samples were sink every day and at the same time for 15-20 minutes into the electrolyte baths for moistening, after which they were lifted and allowed to dry using conditions under which the control group samples were stored. The densities of electrolytes during the experiment were constant and were monitored by a hydrometer. All metal elements on reinforced concrete beams, ensuring the constancy of the design model and the power load magnitude, were coated with anticorrosive compounds. The number of damping-drying cycles was determined by the number of days from the long-time tests beginning to the reinforced concrete beams removal for destruction by a short-time load.

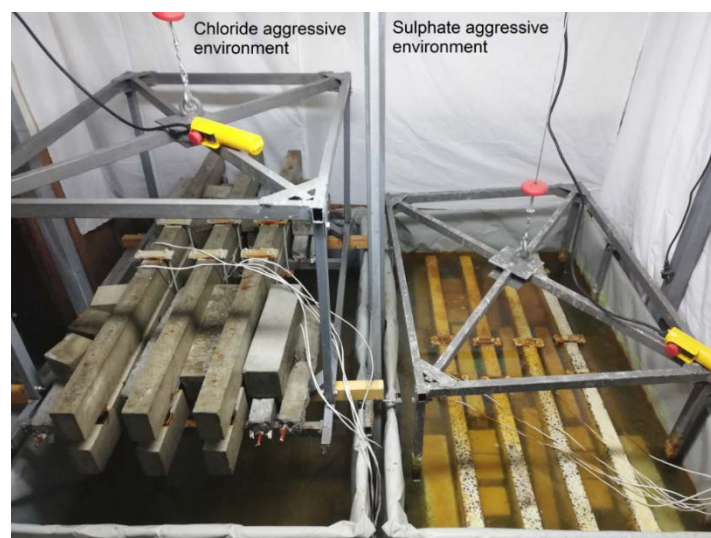


Figure 6. Stand for long-time samples tests.

At the end of long-time tests and samples unloading, the residual values of the deformation characteristics, mass, section sizes were measured, concrete strength was determined by non-destructive methods on all faces.

For reinforced concrete beams tests with a short-time bending load before failure, a test bench was made, the spatial rigidity and stability of which is many times higher than the prototypes rigidity. From the possible types of loading, gravitational piece loads using was adopted. The general tests view is shown in Fig. 7.



Figure 7. General view of reinforced concrete beams test before failure.

The tests were carried out in accordance with Russian State Standard regulations GOST 8829 step loading. At the loading stages preceding the cracks formation and samples fracture, the step size was up to 5 % of the expected breaking load, and at all the other stages was about 10 %. The retention interval at each stage of loading, taking into account the readout from the instruments, was 10-20 minutes. The readings from the measuring instruments were taken twice at each stage – at the end of loading and after loading.

After bringing the beams to failure, various parameters of structural materials corrosion damages were determined. Using the indicator method, by cross section color saturation with a 1 % phenolphthalein solution, the depth at which the concrete properties changes was determined at all its faces. Further, reinforcing bars were removed from the beams, which determined the corrosion depth, weight loss, and the change in the deformation-strength characteristics of steel reinforcement used in the experiment.

3. Results and Discussion

Long-time state of steel reinforcement in concrete. During long-time tests, under influence of aggressive sulfate environment, steel reinforcement in concrete reinforced beams was in a passive state. The absence of corrosion damages of reinforcement can be explained by the limited oxygen access to surface rods due to fracture plugging with concrete corrosion products [11, 31].

During prolonged exposure of a corrosive chloride environment, steel reinforcement corrosion in reinforced concrete beams was initiated. It was determined that with the complete concrete protective properties neutralization, corrosion damages (pittings) in the reinforcement of the greatest depth can be formed on the rod surface that is inverse with respect to the nearest face of the cross section element (Fig. 8).

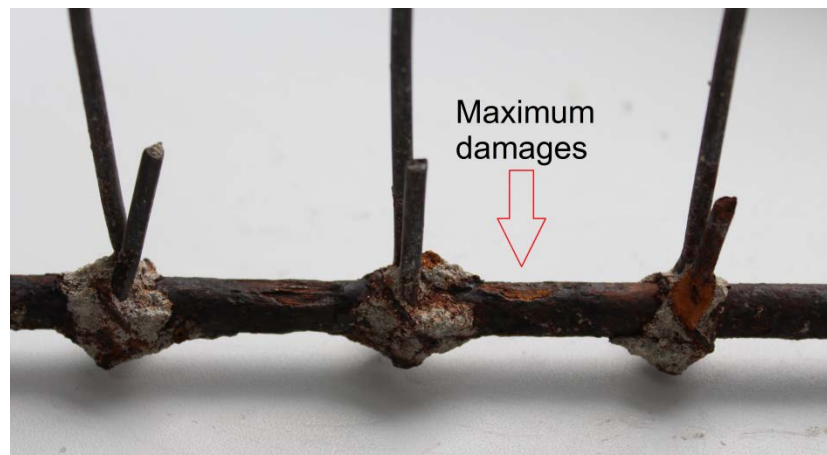


Figure 8. Steel reinforcement corrosion type damages of reinforced concrete beams.

The biggest steel reinforcement damages during chloride aggression were found in sections with operational cracks in concrete. These damages are the closest to the calculated model of uneven corrosion development by the type of "flat front" according to Table. 1.

A graph-based mapping of development rate of corrosion damages to the accepted steel reinforcement during chloride aggression, taking into account the existing stresses, is presented in Fig. 9.

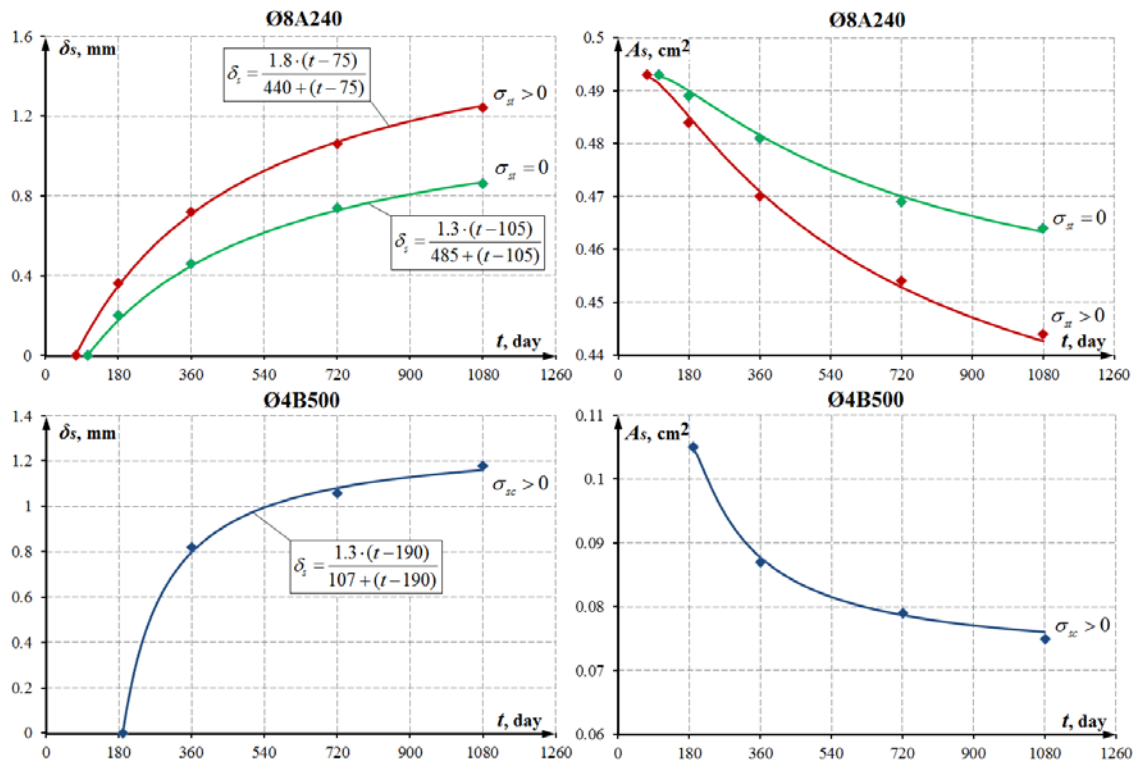


Figure 9. The development rate of steel reinforcement corrosion damages during chloride aggression in depth (left) and in area (right) of the rods cross-section.

Note: in Fig. 9 markers indicate the points, obtained during experimental studies, and the solid lines – calculated curves obtained by the formula (3).

The change nature in deformation diagrams of steel reinforcement obtained by tests of rod samples on axial tension is shown in Fig. 10. After a long-time influence to reinforced concrete beams of an external loading and a chloride aggressive environment, the deformation-strength characteristics of steel reinforcement remained within the limits of variations of the corresponding characteristics of control samples. In this case, like in works [13, 14] a decrease in the length of the yield area is observed.

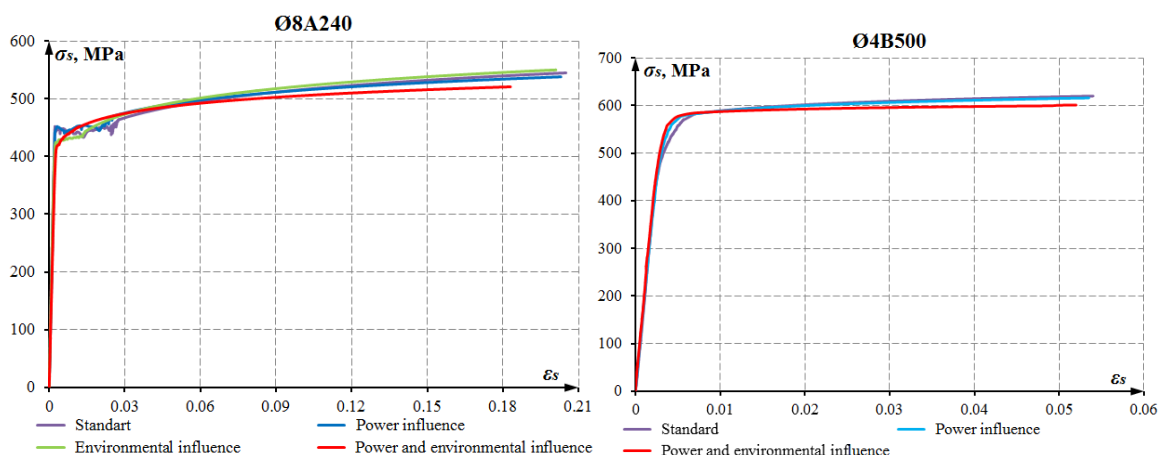


Figure 10. The change nature in the deformation diagrams of steel reinforcement during prolonged power and environmental influences.

Concrete prolonged condition. The concrete corrosion, related with the aggressive effect modeling of chloride on steel reinforcement, proceeded according to the first type, in which salt spots of dissolved cement stone components appeared on the samples surface [7]. Damages accumulation according to the scheme without complete concrete destruction and during the long-time tests was insignificant.

Under the influence of a sulfate-containing aggressive environment, concrete corrosion took place in according to the third form, in which the resulting chemical reaction products settled in the concrete structure, which eventually led to its complete destruction [11]. The corrosion damage accumulation corresponded to the design scheme, which has three zones with different destruction degree. At the same time, in the course of experimental studies it was found that for this scheme the function of the concrete damage coefficient $K^*(z)$ in the transition zone, where the composite resistance is partially preserved, does not take values equal to zero.

The experimental studies results of the concrete state in reinforced concrete beams and unloaded auxiliary samples during various operating environments are presented in Table 3 and Table 4.

Table 3. The concrete strength and deformation characteristics in various operating environments.

Concrete characteristics	Operating environment	Duration of power and environmental influences t , days				
		0	180	360	720	1080
Cube compressive strength R , MPa	Non-aggressive		39.2	39.6	39.9	40.1
	Sulfate	31.0	29.6	28.4	26.9	25.8
	Chloride		38.4	38.9	39.1	38.9
Prism compressive strength R_b , MPa	Non-aggressive		30.4	30.7	30.9	31.0
	Sulfate	23.8	23.7	22.7	21.5	20.6
	Chloride		29.6	29.9	30.0	29.7
Tensile strength R_{bt} , MPa	Non-aggressive		2.9	2.9	3.0	3.0
	Sulfate	2.3	2.4	2.3	2.2	2.2
	Chloride		2.9	2.9	3.0	2.9
Initial modulus of elasticity E_b , MPa	Non-aggressive		35500	35500	36000	36000
	Sulfate	30000	30500	30000	29500	29000
	Chloride		34000	34000	34500	34100
Deformations ε_{bR}	Non-aggressive		0.00190	0.00193	0.00195	0.00195
	Sulfate	0.00180	0.00190	0.00195	0.00200	0.00205
	Chloride		0.00195	0.00200	0.00205	0.00210

Table 4. Kinetics characteristics of concrete corrosion damages in various operating environments.

Concrete damages characteristics	Aggressive environment	Concrete stress	Duration of power and environmental influences t , days				
			0	180	360	720	1080
Corrosion damage depth δ , mm (including completely destroyed concrete layer thickness)	Sulfate	$\sigma_{bt} \approx R_{bt}$		6.5 (1.8)	10.5 (2.4)	12.5 (2.8)	13 (3.1)
		$\sigma_b = 0$	0	5 (1.6)	7.5 (2.1)	9 (2.4)	9.5 (2.6)
		$\sigma_b = 0.55R_b$		3.5 (1.4)	5 (1.9)	5.5 (2.2)	5.5 (2.4)
	Chloride	$\sigma_{bt} \approx R_{bt}$		17	21	22	22.5
		$\sigma_b = 0$	0	14	17.5	19	19
Damage coefficient K_{\min}^*	Sulfate	-	1	0.78	0.74	0.70	0.67
	Chloride	-		0.97	0.97	0.97	0.96

According to the data obtained, the change in the strength and deformation characteristics of concrete and corrosion damage development in it with time depends on the operating environment type, the sign and level of acting stresses. The concrete properties greatest degradation is observed under the sulfate aggressive environment influence. The maximum and minimum depth of concrete corrosion damage is determined respectively in the stretched and compressed zones of the sections of reinforced concrete beams. The concrete damages in unloaded auxiliary samples and in beams at the neutral axis level was approximately equal (Fig. 11, a, b). The corrosion frontal advance to the deep into the concrete was uniform at all faces, with the exception of cross sections side faces of the bent elements, where the sign and level of stress changes in height.

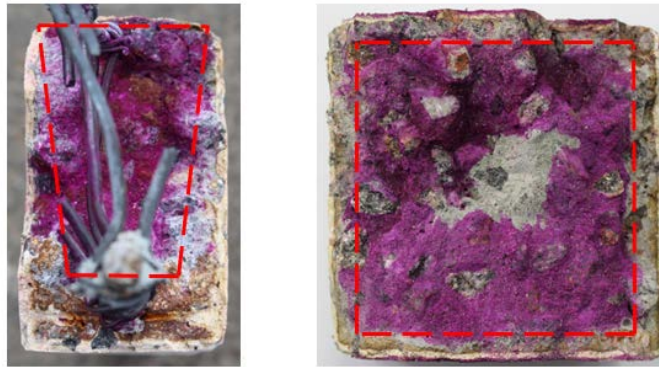


Figure 11. The nature of corrosion damages development in concrete of reinforced concrete beams (a) and unloaded auxiliary samples (b).

A graphic representation of the corrosion damages development rate in concrete under various operating environments is shown in Fig. 12. It should be noted that concrete damages accumulated under sulfate-containing environment influence at a lower development depth have a higher destruction degree than damages received in a chloride-containing environment. Herewith, both types of concrete damages have a damping in time character.

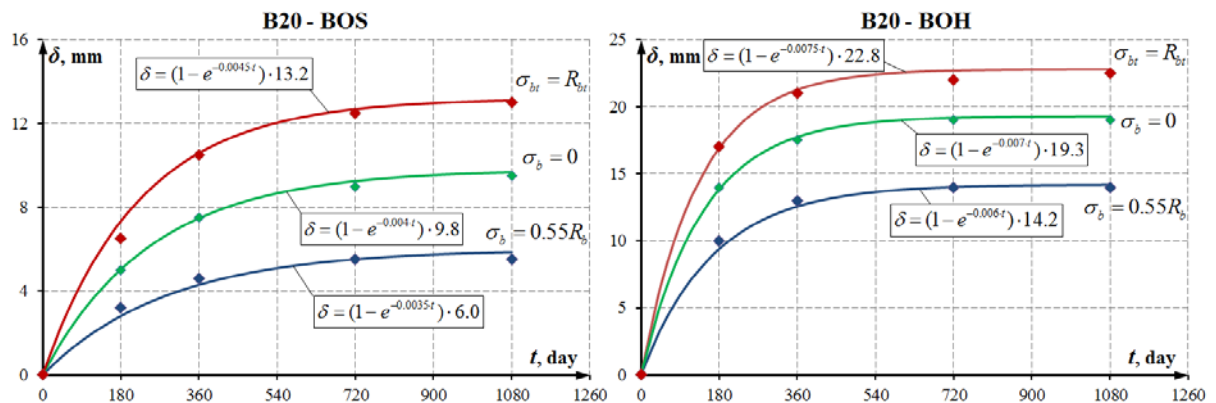


Figure 12. The corrosion damages development rate in concrete of class B20 with liquid sulfate (left) and chloride (right) aggression.

Note: in Fig. 12, the markers indicate the points obtained during the experimental studies, and the solid lines – calculated curves obtained by the formula (1).

Adhesion condition of reinforcement with concrete. The deformations development in concrete and tensile reinforcement in the area between cracks at different levels of beam loading is shown as an example in Fig. 13, from which it can be seen that until the ratio $P/P_u \approx 0.85$, it proceeded at approximately the same rate (deviations do not exceed 25 %). At the stage preceding the samples destruction, a partial breaking in the concrete and reinforcement deformation can be neglected due to many factors affecting the readings of tensiometers, and structural materials deformation as a whole can be considered the same with an acceptable error.

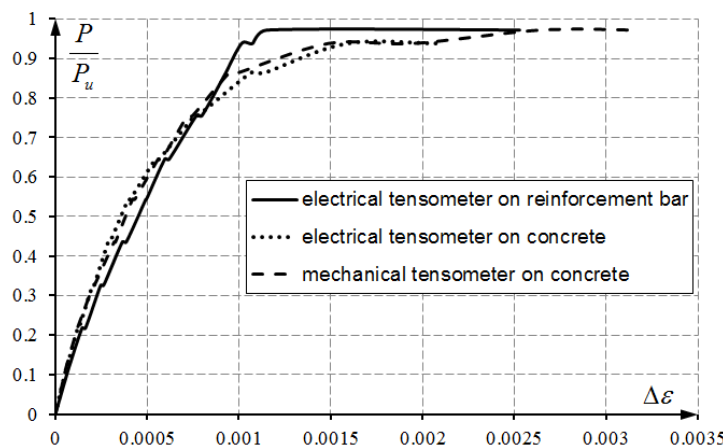


Figure 13. Deformations in tensile concrete and reinforcement.

Bendable reinforced concrete elements. The destruction of all reinforced concrete beams samples during load tests in the form of two concentrated forces occurred in the zone of pure bending along normal sections. The values of breaking loads are given in Table 5.

Table 5. The breaking loads values during reinforced concrete beams testing.

Duration of power and environmental influences before failure testing t , days	Control group (Non-aggressive environment)		Main group no. 1 (Sulphate-aggressive environment)		Main group no. 2 (Chloride-aggressive environment)	
	Sample marking	Breaking load, kN	Sample marking	Breaking load, kN	Sample marking	Breaking load, kN
0	BK-0-1	6.273	-	-	-	-
	BK-0-2	6.292	-	-	-	-
	BK-0-3	6.281	-	-	-	-
180	BK-180-1	6.383	BOS-180-1	6.222	BOH-180-1	6.229
	BK-180-2	6.360	BOS-180-2	6.191	BOH-180-2	6.203
360	BK-360-1	6.371	BOS-360-1	6.099	BOH-360-1	6.046
	BK-360-2	6.391	BOS-360-2	6.140	BOH-360-2	6.012
720	BK-720-1	6.381	BOS-720-1	6.024	BOH-720-1	5.846
	BK-720-2	6.402	BOS-720-2	6.068	BOH-720-2	5.868
1080	BK-1080-1	6.390	BOS-1080-1	6.038	BOH-1080-1	5.701
	BK-1080-2	6.414	BOS-1080-2	5.968	BOH-1080-2	5.609

For control group samples, an increase in the breaking load with time up approximately 2 % was observed, which is associated with concrete strength increasing by 30 %.

All samples of the main groups are characterized by a decrease in bearing capacity with an increase in the period of environmental impacts and corrosion damages accumulation in structural materials. After 1080 days, for beams that were in sulfate and chloride-containing aggressive environment, when compared with control beams of the same time, the breaking load decreased on average by 6.6 % and 13.2 %, respectively. Thus, with the same structural features, the beams strength with steel reinforcement corrosion damage decreases more than with concrete damage. This effect is coordinated with research results [5, 8, 12, 16, 17].

The general diagram of reinforced concrete beams destructive loads changes with the time is shown in Fig. 14.

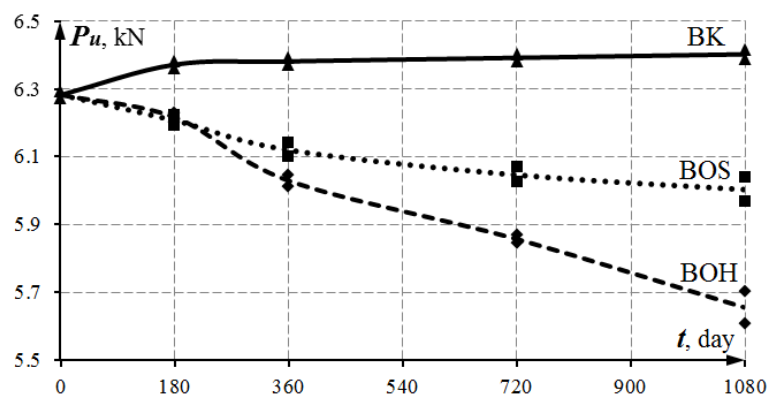


Figure 14. The change in the beams breaking load with the time.

In order to numerical realization of the developed design procedure, a calculation algorithm was formulated and computer program was written. Using them, the theoretical values of normal sections strength adopted for samples experimental studies of reinforced concrete beams are determined.

To compare with the theoretical values of the normal sections strength determined by the developed design procedure, the actual ultimate breaking loads values for each series of reinforced concrete beams samples tests were averaged and, in accordance with the design scheme, are presented as experimental values of the normal sections strength (Table 6). The average deviation between the corresponding experimental and calculated values of strength is about 1.5 %, the maximum deviation does not exceed

3 %. The root-mean-square deviation range does not exceed 1 %. Herewith, all calculated values do not exceed the experimental ones.

Table 6. Experimental and calculated values comparison of normal sections strength of reinforced concrete beams samples.

Samples series	Normal section strength M_u , kN·m		
	Observation value M_u^{obs}	Calculated value M_u^{cal}	$\frac{M_u^{cal}}{M_u^{obs}}$
Non-aggressive operating environment (the control group samples)			
BK-0	1.837	1.800	0.980
BK-180	1.864	1.844	0.989
BK-360	1.866	1.845	0.989
BK-720	1.870	1.848	0.988
BK-1080	1.873	1.849	0.987
Samples group average			0.987
Samples group root-mean-square deviation			0.0038
Sulphate-containing aggressive environment (samples of main group no. 1)			
BOS-180	1.816	1.772	0.976
BOS-360	1.790	1.754	0.980
BOS-720	1.769	1.745	0.986
BOS-1080	1.756	1.739	0.990
Samples group average			0.983
Samples group root-mean-square deviation			0.0062
Chloride-containing aggressive environment (samples of main group no. 2)			
BOH-180	1.818	1.796	0.988
BOH-360	1.764	1.730	0.981
BOH-720	1.713	1.679	0.980
BOH-1080	1.655	1.632	0.986
Samples group average			0.984
Samples group root-mean-square deviation			0.0039
Average of all samples			0.985
Root-mean-square deviation of all samples			0.0046

4. Conclusions

Based on the study results, taking into account the tasks, the following conclusions can be made:

1. Based on reinforced concrete deformation model, a universal method has been developed for strength calculating of normal sections of flexible reinforced concrete elements subject to prolonged force and environmental influences. It allows to take into account the concrete nonlinear deformation, various schemes of corrosion damage forming within the rectangular cross section, as well as various degrees of sections damage within the span.

2. New experimental data of normal sections strength of reinforced concrete beams samples that have been under stress in sulfate- and chloride-containing aggressive environments for a long time were obtained. For samples with corrosion damage of concrete and reinforcement compared to control samples, a decrease in the bearing capacity with an increase in the exposure time of an aggressive environment is characteristic. For samples with concrete and reinforcement corrosion damages as compared to control samples, a decrease in the bearing capacity with an increase in the exposure time of aggressive environment is characteristic. It was found that during sulfate aggression, the concrete damage coefficient function in the transition zone does not take values equal to zero. With chloride aggression and complete neutralization of concrete protective properties, pittings of the maximum depth can be formed on the reinforcement bar surface that is inverse to the nearest face of the element section.

3. A comparison of the experimental and calculated data on the strength of normal sections was carried out, which showed that the calculation method proposed in the work has sufficient accuracy and can be used for practical calculations of operated and newly designed flexible concrete elements taking into account manufacturing defects and corrosion damages accumulation to structural materials over time.

References

1. Ma, Y., Xiang, Y., Wang, L., Zhang, J., Liu, Y. Fatigue life prediction for aging RC beams considering corrosive environments. *Engineering Structures*. 2014. No. 79. Pp. 211–221. DOI: 10.1016/j.engstruct.2014.07.039
2. Adhikary, S.D., Li, B., Fujikake, K. Dynamic behavior of reinforced concrete beams under varying rates of concentrated loading. *International Journal of Impact Engineering*. 2012. No. 47. Pp. 24–38. DOI: 10.1016/j.ijimpeng.2012.02.001
3. Ye, H., Fu, C., Jin, N., Jin, X. Performance of reinforced concrete beams corroded under sustained service loads: A comparative study of two accelerated corrosion techniques. *Construction and Building Materials*. 2018. No. 162. Pp. 286–297. DOI: 10.1016/j.conbuildmat.2017.10.108
4. Zhang, W., Zhang, H., Gu, X., Liu, W. Structural behavior of corroded reinforced concrete beams under sustained loading. *Construction and Building Materials*. 2018. No. 174. Pp. 675–683. DOI: 10.1016/j.conbuildmat.2018.04.145
5. Bossio, A., Imperatore, S., Kioumarsis, M. Ultimate flexural capacity of reinforced concrete elements damaged by corrosion. *Buildings*. 2019. 9(7). P. 160. DOI: 10.3390/buildings9070160
6. Du, Y., Cullen, M., Li, C. Structural effects of simultaneous loading and reinforcement corrosion on performance of concrete beams. *Construction and Building Materials*. 2013. No. 39. Pp. 148–152. DOI: 10.1016/j.conbuildmat.2012.05.006
7. Yu, L., Francois, R., Dang, V.H., L'Hostis, V., Gagne, R. Structural performance of RC beams damaged by natural corrosion under sustained loading in a chloride environment. *Engineering Structures*. 2015. No. 96. Pp. 30–40. DOI: 10.1016/j.engstruct.2015.04.001
8. Hanjari, K.Z., Kettil, P., Lundgren, K. Analysis of mechanical behavior of corroded reinforced concrete structures. *Aci Structural Journal*. 2011. 108(5) Pp. 532–541.
9. Zhao, Y., Yu, J., Jin, W. Damage analysis and cracking model of reinforced concrete structures with rebar corrosion. *Corrosion Science*. 2011. 53(10). Pp. 3388–3397. DOI: 10.1016/j.corsci.2011.06.018
10. Otieno, M.B., Alexander, M.G., Beushausen, H.-D. Corrosion in cracked and uncracked concrete – influence of crack width, concrete quality and crack reopening. *Magazine of Concrete Research*. 2010. 62(6). Pp. 393–404. DOI: 10.1680/mac.2010.62.6.393
11. Okeniyi, J.O., Omotosho, O.A., Ajayi, O.O., Loto, C.A. Effect of potassium-chromate and sodium-nitrite on concrete steel-rebar degradation in sulphate and saline media. *Construction and Building Materials*. 2014. No. 50. Pp. 448–456. DOI: 10.1016/j.conbuildmat.2013.09.063
12. Zhu, W., Francois, R., Coronelli, D., Cleland, D. Effect of corrosion of reinforcement on the mechanical behaviour of highly corroded RC beams. *Engineering Structures*. 2013. No. 56. Pp. 544–554. DOI: 10.1016/j.engstruct.2013.04.017
13. Boubitsas, D., Tang, L. The influence of reinforcement steel surface condition on initiation of chloride induced corrosion. *Materials and Structures*. 2015. 48(8). Pp. 2641–2658. DOI: 10.1617/s11527-014-0343-2
14. Pradhan, B. Corrosion behavior of steel reinforcement in concrete exposed to composite chloride-sulfate environment. *Construction and Building Materials*. 2014. No. 72. Pp. 398–410. DOI: 10.1016/j.conbuildmat.2014.09.026
15. Stewart, M.G., Suo, Q. Extent of spatially variable corrosion damage as an indicator of strength and time-dependent reliability of RC beams. *Engineering Structures*. 2009. 31(1). Pp. 198–207. DOI: 10.1016/j.engstruct.2008.08.011
16. Xia, J., Jin, W.-L., Li, L.-Y. Effect of chloride-induced reinforcing steel corrosion on the flexural strength of reinforced concrete beams. *Magazine of Concrete Research*. 2012. 64(6). Pp. 471–485. DOI: 10.1680/mac.10.00169
17. Zhu, W., Francois, R. Corrosion of the reinforcement and its influence on the residual structural performance of a 26-year-old corroded RC beam. *Construction and Building Materials*. 2014. No. 51. Pp. 461–472. DOI: 10.1016/j.conbuildmat.2013.11.015
18. Shamshina, K.V., Migunov, V.N., Ovchinnikov, I.G. Influence of corrosion longitudinal cracks on rigidity and strength of reinforced concrete structures. *IOP Conference Series: Materials Science and Engineering*. 2018. 451(1). P. 012058. DOI: 10.1088/1757-899X/451/1/012058
19. Kivell, A., Palermo, A., Scott, A. Complete model of corrosion-degraded cyclic bond performance in reinforced concrete. *Journal of Structural Engineering (United States)*. 2014. 141(9). P. 04014222. DOI: 10.1061/(ASCE)ST.1943-541X.0001195
20. Bondarenko, V.M., Kolchunov, V.I. Kontsepsiya i napravleniya razvitiya teorii konstruktivnoy bezopasnosti zdaniy i sooruzheniy pri silovykh i sredovykh vozdeystviyakh [The concept and directions of development of the theory of structural safety of buildings and structures under the influence of force and environmental factors]. *Industrial and Civil Engineering*. 2013. No. 2. Pp. 28–31. (rus)
21. Ababneh, A., Sheban, M. Impact of mechanical loading on the corrosion of steel reinforcement in concrete structures. *Materials and Structures/Materiaux et Constructions*. 2011. 44(6). Pp. 1123–1137. DOI: 10.1617/s11527-010-9688-3
22. Wang, X.-H., Liu, X.-L. Simplified methodology for the evaluation of the residual strength of corroded reinforced concrete beams. *Journal of Performance of Constructed Facilities*. 2010. 24(2). Pp. 108–119. DOI: 10.1061/(ASCE)CF.1943-5509.0000083
23. Selyayev, V.P., Bondarenko, V.M., Selyayev, P.V. Prognozirovaniye resursa zhelezobetonnykh izgibayemykh elementov, rabotayushchikh v agressivnoy srede, po pervoy stadii predelnykh sostoyaniy [Forecasting the service life (resource) of reinforced concrete bending elements working in aggressive environment at the first stage of limit states]. *Regional Architecture and Engineering*. 2017. 2(31). Pp. 14–24. (rus)
24. Coronelli, D., Gambarova, P. Structural assessment of corroded reinforced concrete beams: Modeling guidelines. *Journal of Structural Engineering*. 2004. 130(8). Pp. 1214–1224. DOI: 10.1061/(ASCE)0733-9445(2004)130:8(1214)
25. Torres-Acosta, A.A., Navarro-Gutierrez, S., Teran-Guillen, J. Residual flexure capacity of corroded reinforced concrete beams. *Engineering Structures*. 2007. 29(6). Pp. 1145–1152. DOI: 10.1016/j.engstruct.2006.07.018
26. Karpenko, N.I., Karpenko, S.N., Yarmakovskiy, V.N., Yerofeyev, V.T. O sovremennykh metodakh obespecheniya dolgovechnosti zhelezobetonnykh konstruksiy [The modern methods for ensuring of the reinforced concrete structures durability]. *Academia. Architecture and Construction*. 2015. No. 1. Pp. 93–102. (rus)
27. Murashkin, G.V., Pischulev, A.A. Using deformation models to determine the bearing capacity of reinforced concrete flexural members with corrosion damages of concrete compressed zone. *Building and reconstruction*. 2009. No. 6. P. 36. (rus)
28. Alfarah, B., Lopez-Almansa, F., Oller, S. New methodology for calculating damage variables evolution in Plastic Damage Model for RC structures. *Engineering Structures*. 2017. No. 32. Pp. 70–86. DOI: 10.1016/j.engstruct.2016.11.022
29. Chen, H., Nepal, J. Modeling residual flexural strength of corroded reinforced concrete beams. *Aci Structural Journal*. 2018. 115(6). Pp. 1625–1635. DOI: 10.14359/51702232

30. Kolchunov, V.I., Kolchunov, V.I., Fedorova, N.V. Deformatsionnyye modeli zhelezobetona pri osobykh vozdeystviyakh [Deformation models of reinforced concrete under special impacts]. Industrial and Civil Engineering. 2018. No. 8. Pp. 54–60. (rus)
31. Fedosov, S.V., Rumyantseva, V.E., Krasilnikov, I.V., Konovalova, V.S., Evsyakov, A.S. Mathematical modeling of the colmatation of concrete pores during corrosion. Magazine of Civil Engineering. 2018. 83(7). Pp. 198–207. DOI: 10.18720/MCE.83.18
32. Kryuchkov, A.A., Smolyago, G.A., Zhdanov, A.Ye. Issledovaniye napryazhenno-deformirovannogo sostoyaniya zhelezobetonnykh sterzhnevykh elementov s uchetom vliyaniya poperechnoy sily [Investigation of the stress-strain state of reinforced concrete core elements taking into account the influence of shear force]. Bulletin of BSTU named after. V.G. Shukhov. 2005. No. 10. Pp. 449–451. (rus)
33. Sazonov, E.V., Shmelev, G.D., Ishkov, A.N. Prakticheskie aspekty ispolzovaniya parametricheskikh metodov otsenki ostatochnogo resursa dlya plit pokrytiya [Practical aspects of using parametric methods of residual life assessment for roof slabs]. News of higher educational institutions. Construction. 2007. 557(1). Pp. 15–20. (rus)

Contacts:

Nikolay Frolov, frolov_pgs@mail.ru

Gennady Smolyago, tpk-psv@yandex.ru

© Frolov, N.V., Smolyago, G.A., 2021